ARTICLE

OBC
www.rsc.org/obc

An experimental and theoretical study on the substituent effect of the permanganate oxidation of styrenes †

Toshio Ogino,* Hisashi Yaezawa, Osamu Yoshida and Mayumi Ono
Department of Chemistry, Faculty of Education and Human Science, Niigata University, Niigata 950-2181, Japan. E-mail: ogino@ed.niigata-u.ac.jp; Fax: +81-25-262-7152; Tel: +81-025-262-7152

Received 11th March 2003, Accepted 16th June 2003
First published as an Advance Article on the web 7th July 2003

The kinetic data obtained for the cycloadditions of the permanganate ion to a series of styrene derivatives in dichloromethane solution in the presence of a quaternary ammonium ion were examined with two theoretical approaches, on the assumption that the reactions proceed *via* a concerted [3 + 2] mechanism. The semi-quantitative frontier molecular orbital analysis of the kinetic data shows a linear free energy relationship with better correlation than the Hammett plot with σ values when the point for *p*-NO_2 group is omitted. Further examination of the results of the FMO analysis reveals that the deviation of the point for *p*-nitrostyrene is attributed to the transition structure being more reactant-like than that of the other derivatives. The plot of log k_2 *vs.* $-\Delta G^{\ddagger}$ calculated by the density functional theory (Becke3LYP) follows a straight line with the desired correlation for all the substituents. A marked tendency was observed for the MO calculations to underestimate the $\Delta G^{\ddagger}$ value for electron-withdrawing substituents when the calculation was carried out excluding the quaternary ammonium ion. This inconsistency was much improved by the calculations incorporating the quaternary ammonium ion. The actual values of $\Delta G^{\ddagger}$ obtained from the Eyring analysis are in good agreement with those calculated at the B3LYP/6-311+G(d,p)//B3LYP/LanL2DZ level.

Introduction

It has been accepted since the end of the 19th century that permanganate oxidation of alkenes proceeds *via* the transient cyclic manganate(v) ester intermediate **1** (Scheme 1).[1] There have been two kinds of discussion concerning the mechanism of this reaction in the last quarter of the 20th century. The first is related to the question of whether a manganese intermediate spectrophotometrically observed during the reactions in organic solution in the presence of a quaternary ammonium ion or in weakly acidic buffer solution is the intermediate **1** itself or not.[2] The other, more contemporary controversy is related to the mechanism of the cycloaddition step.

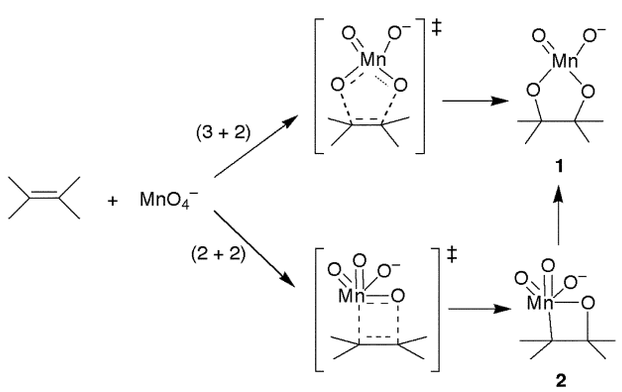

Scheme 1 Two pathways for permanganate addition to alkene.

Two different pathways, both of which lead to the intermediate **1**, have been proposed (Scheme 1). The concerted [3 + 2] pathway, which involves a five-membered transition state, was theoretically suggested on the basis of the frontier molecular orbital (FMO) theory[3] and the Zimmerman treatment.[4] On the other hand, the [2 + 2] pathway in which a metallaoxetane intermediate **2** is initially formed and then rearranges to **1** is based on the general proposal for reactions of oxo-transition metal reagents with alkenes by Sharpless *et al.*[5] Similar topics have been discussed coincidentally for the reactions between OsO_4 and alkenes.[6]

In a previous paper,[7] we have shown that the experimentally observed substituent effects of various types of alkenes on permanganate oxidation are semi-quantitatively explicable on the assumption of the [3 + 2] mechanism by using a rate equation derived from the general perturbation equation and the FMO theory. More recently, it has been shown that the free energies of activation of the [3 + 2] pathway calculated according to the density functional theory for the permanganate oxidation of ethylene and a series of alkenoic acids are 160 to 190 kJ mol^{-1} lower than that of the [2 + 2] pathway.[8] Similar results have been reported also for the reactions of OsO_4.[9]

Although the [3 + 2] mechanism is favored by direct theoretical calculations, the existing studies have been limited to small molecules and very little comparison with experimental data has been conducted to date. In this paper, in order to clarify the [3 + 2] mechanism in more detail, we have performed kinetic experiments for the reactions of styrene derivatives in organic solution in the presence of a quaternary ammonium ion, and then analysed the results using two theoretical approaches. First, we examined the linear free energy relationship of the kinetic results using the semi-quantitative FMO method,[7] which is employable instead of the Hammett analysis with high enough accuracy using semi-empirical MO calculations. Second, we calculated the Gibbs free energies of activation ($\Delta G^{\ddagger}$) for the reactions of all the derivatives using density functional theory (DFT), and compared the resulting values with those obtained from an Eyring plot of the kinetic results. Although several kinetic studies on the substituent effects of aryl alkenes have been done to explore the cycloaddition step of the permanganate oxidation,[2c,2d,10] we chose here the reaction of simple styrene derivatives in order to avoid the difficulty in computing large and complex molecules.

† Electronic supplementary information (ESI) available: Additional data. See http://www.rsc.org/suppdata/ob/b3/b302693k/

DOI: 10.1039/b302693k

Experimental

p-Chloro, *m*-nitro, *p*-nitro and non-substituted styrene were purchased from Tokyo Kasei Kogyo Co., Ltd. (Tokyo, Japan), and *p*-methylstyrene from Wako Pure Chemical Industries, Ltd. (Osaka, Japan) and were used without any purification. *m*-Chloro, *m*-bromo, and 3,4-dichlorostyrene were prepared according to the standard method described in the literature.[11]

The kinetic experiments were performed using a spectrometer for the reaction between a styrene derivative and permanganate ion solubilised in dichloromethane by use of tetraethylammonium chloride. The permanganate solutions were prepared in a similar manner previously described[2g,7] and the accurate concentration was spectrophotometrically determined immediately before use. The reactions were performed by mixing a dichloromethane solution of permanganate ion (2 mL, *ca.* 2×10^{-4} mol L) and a dichloromethane solution of a styrene (2 mL, *ca.* $2–7 \times 10^{-4}$ mol L^{-1}) in a 10 mm cuvette. The kinetics were determined by monitoring the changes in absorbance at 526 nm (disappearance of permanganate ion). The temperature was maintained at 25.0 °C with a refrigerated and heated bath circulator. The absorbance data were corrected at each time by subtracting the increasing background at this wavelength (due to the formation of manganese intermediate) estimated from the observed absorbance at 420 nm, where the reactants have no absorption.

All the rate constants (k_2) are the average of four or more times experimental. Activation parameters for the permanganate reactions of all the styrene derivatives were determined from the plots of ln k_2/T *vs.* $1/T$ using k_2 values determined at 15.0, 20.0, 25.0, and 30.0 °C, respectively.

Computational procedure

DFT (Becke3LYP)[12] calculations were performed using the program Gaussian 98.[13] Geometry optimizations were carried out using two levels of DFT calculations, B3LYP/LanL2DZ[14] and B3LYP/6-31G(d). Frequency calculations were also performed at these levels and it was verified that each structure corresponds to a minimum or transition state. The frequencies used for the computation of the thermal corrections to Gibbs energy and entropy calculations were scaled by 0.9804[15] for the calculations at the B3LYP/6-31G(d) but not scaled for the calculations at the B3LYP/LanL2DZ level. For these optimised geometries the energies are also evaluated at the level of B3LYP/6-311+G(d,p). Gibbs free energies of activation ($\Delta G^{\ddagger}$) at the 6-311+G(d,p) level are calculated based on the electronic energies at this level and the thermal corrections calculated at the optimization level. Orbital energies and eigenvectors of the styrenes used for the FMO analysis were calculated by PM3[16] in MOPAC 97. The HOMO energy of permanganate, −8.5 eV, was adopted based on the value obtained by the PM3(tm) method[17] in the program suit Mac Spartan 1.2[18] and an empirical correction.[7]

Results and discussion

Semi-quantitative FMO analysis

Fig. 1 shows the results of the kinetic measurements in the form of a Hammett plot against σ values. An excellent straight line

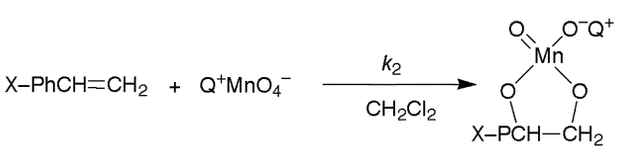

with positive slope ($\rho = 0.76$) is obtained when *p*-nitrostyrene is omitted from the plot. The upward deviation of *p*-nitrostyrene from the straight line is corrected, however, by adopting a σ^-

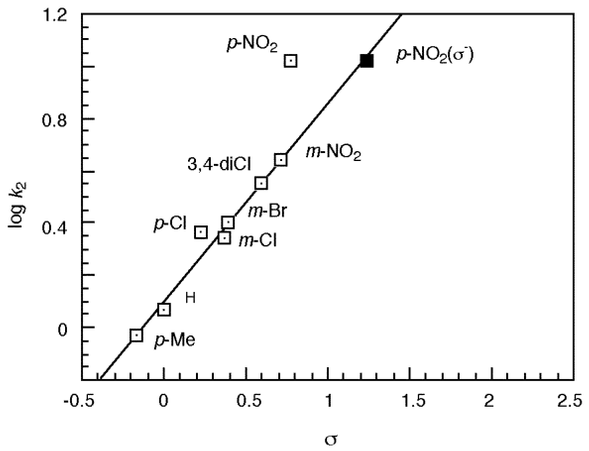

Fig. 1 Hammett plot for the reactions of $MnO_4^-Q^+$ with substituted styrenes in CH_2Cl_2; $\rho = 0.76$, $r = 0.98$.

value for *p*-NO_2 group. These facts indicate that the reactions involve a nucleophilic attack of permanganate ion in the rate-determining step and the electron-withdrawing resonance effect lowers the transition energy particularly in the reaction of *p*-nitrostyrene.

We examined the kinetic data by the semi-quantitative FMO method using the following equation (eqn. 1) we proposed previously.[7] This equation provides a simple theoretical method to evaluate the linear free energy relationship of the rate constant (k_2) for a concerted cycloaddition reaction based on the general perturbation theory.[19]

$$\ln k_2 \propto C + \frac{2\beta^2 C_{RH}^2}{RT}\left[\frac{(1-d)\left(|C_{SL1}| + |C_{SL2}|\right)^2 + 2d}{|E_{RH} - E_{SL}|}\right] \qquad (1)$$

The right hand side of eqn. 1 represents the magnitude of energy stabilization caused by the HOMO–LUMO interaction in a concerted cycloaddition reaction where the donor component is symmetric as MnO_4^-. C_{SL1} and C_{SL2} represent the eigenvectors of LUMO at the atoms of the reaction site of the unsymmetrical acceptor, *i.e.*, styrenes in this case, and $E_{RH} - E_{SL}$ denotes the HOMO–LUMO energy difference between the donor and acceptor. The parameter *d* varies from 0 to 1 with the location of the transition state along the reaction coordinate and is concerned with the extent of equalization and localization of lobes extending at the atoms of the reaction site. Thus, if one can determine the right value of *d* for a series of related cycloaddition reactions where transition structures are similar, a linear relationship could be expected between ln k_2 and the values calculated for the terms in brackets in eqn. 1. Semi-empirical MO calculations usually give correlation coefficients (*r*) as good as those of Hammet plots for the cycloaddtion reactions such as Diels–Alder reactions.[7] Table 1 shows the MO data required for this analysis together with the experimental rate data.

An excellent straight line ($r = 0.998$) very similar to that of the Hammett plot results when *d* is taken as 0.74 for all the derivatives except *p*-nitrostyrene which deviates strongly downward (Fig. 2). This deviation suggests that the nature of the transition state in the reaction of *p*-ntirostyrene is not similar to those of other styrenes, and hence the same *d* value cannot apply to its reaction. When *d* is taken as 0.70 instead of 0.74 for *p*-nitrostyrene, the point for *p*-nitrostyrene moves onto the straight line as shown in Fig. 2. According to the definition of *d*, this suggests that the transition structure for *p*-nitrostyrene is more reactant-like than those of other styrene derivatives. It should be noted that the deviation of *p*-nitrostyrene observed in the Hammett plot with σ values and that in the FMO plot move

Table 1 Second-order rate constants[a] for permanganate reactions and semiempirical MO data[b] for styrene derivatives

X	k_2/mol^{-1} L s^{-1}	E_{SL}/eV	Eigen vectors C_{SL1}	Eigen vectors C_{SL2}
p-Me	0.93 ± 0.01	−0.120	0.2995	−0.4433
H	1.18 ± 0.01	−0.122	0.3088	−0.4542
p-Cl	2.31 ± 0.10	−0.375	−0.2743	0.4270
m-Cl	2.19 ± 0.06	−0.326	0.2864	−0.4387
m-Br	2.55 ± 0.04	−0.385	−0.2825	0.4372
3,4-diCl	3.55 ± 0.06	−0.536	−0.2548	0.4120
m-NO2	4.38 ± 0.08	−0.703	−0.2305	0.3584
p-NO2	10.52 ± 0.15	−1.351	0.1718	−0.3496

[a] Determined at 25 °C. [b] Calculated by PM3 in MOPAC 97 on the structures optimised at the same level.

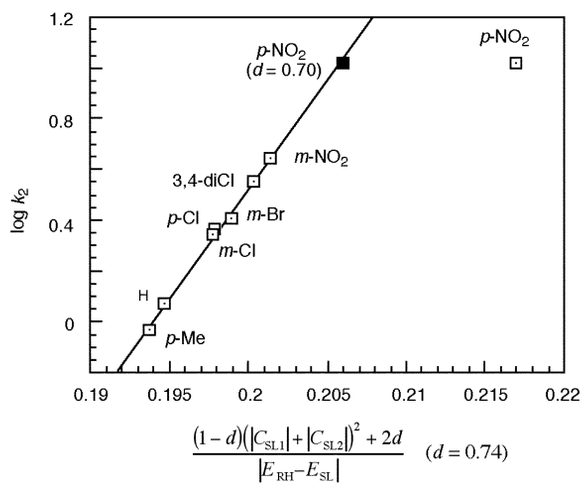

Fig. 2 Plots of log k_2 *vs.* $[(1 - d)(|C_{SL1}| + |C_{SL2}|)^2 + 2d]/|E_{RH} - E_{SL}|$ for the reactions of $MnO4^-$ with substituted styrenes; $d = 0.74$, $r = 0.998$.

in opposite directions. The upward deviation in the Hammett plot is due to the fact that σ values are defined on the basis of acidity constants of benzoic acids in which the resonance effect of the *p*-NO_2 group is not involved, and hence the σ value underestimates the reactivity of *p*-nitrosyrene. On the other hand, in the FMO analysis the resonance effect in the ground state of *p*-nitrostyrene is taken into account from the first, but it is less significant in the transition state because of the change in hybridization from sp^2 to sp^3 at the reaction site. Consequently, the calculation for *p*-nitrostyrene using eqn. 1 tends to overestimate the reactivity and causes a downward deviation when we use the same *d* value as that used for other styrene derivatives, for which the resonance effect is not critical, neither in the ground state nor in the transition state.

Transition states calculated without a quaternary ammonium ion

We first calculated structures and energies ignoring the presence of a quaternary ammonium ion in the reactants and transition states. Structure optimizations and frequency calculations were carried out at the level of B3LYP/LanL2DZ and B3LYP/6-31G(d), and single-point energy calculations at the B3LYP/6-311+G(d,p) level were performed on these optimised structures.

In Table 2, some structural features of the calculated transition states are listed. As predicted in the above discussion on the FMO plot (Fig. 2), all the transition structures are similar to each other except that of *p*-nitrostyrene. The long distance of C1–O1 and the small dihedral angle of C2–C1–C1′–C2′ observed for *p*-nitrostyrene are in good agreement with the above prediction that the transition structure for *p*-nitrostyrene is more reactant-like. Since the *d* value is considered to be an

Table 2 Bond distances and dihedral angles in transition states optimised at B3LYP/LanL2DZ and B3LYP/6-31G(d) without a tetraethylammonium ion[a]

X	Bond distance/Å C1–O1	C2–O2	C1–C2	Dihedral angle/° C2–C1–C1′–C2′
p-Me	2.27 (2.25)	2.07 (1.94)	1.39 (1.39)	−24.4 (−26.7)
H	2.27 (2.25)	2.07 (1.94)	1.39 (1.39)	−23.8 (−26.6)
p-Cl	2.29 (2.27)	2.07 (1.93)	1.39 (1.39)	−24.0 (−25.7)
m-Cl	2.29 (2.27)	2.07 (1.93)	1.39 (1.39)	−24.7 (−26.2)
m-Br	2.29 (2.27)	2.07 (1.93)	1.39 (1.39)	−25.7 (−26.9)
3,4-diCl	2.29 (2.28)	2.07 (1.93)	1.39 (1.39)	−24.9 (−26.8)
m-NO_2	2.29 (2.27)	2.07 (1.93)	1.39 (1.39)	−28.4 (−29.2)
p-NO_2	2.40 (2.37)	2.06 (1.92)	1.39 (1.39)	−15.7 (−21.5)

[a] Figures in parenthesis are the values for B3LYP/6-31G(d) optimised structure.

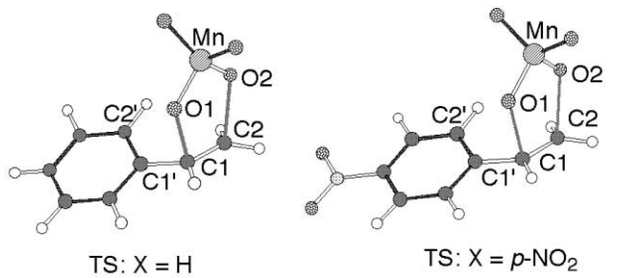

Table 3 Free energies of activation for [3 + 2] addition of MnO_4^- to X–PhCH=CH_2 calculated excluding a quaternary ammonium ion (in kJ mol^{-1} at 298.15 K)

X	$\Delta G^{\ddagger}$[a] B3LYP/6-311+G(d,p) // B3LYP/LanL2DZ	$\Delta G^{\ddagger}$[a] B3LYP/6-311+G(d,p) // B3LYP/6-31G(d)
p-Me	87.4	92.9
H	84.9	89.9
p-Cl	72.1	77.3
m-Cl	71.1	76.1
m-Br	69.2	74.6
3,4-diCl	61.9	67.6
m-NO_2	52.2	57.8
p-NO_2	40.7	49.7

[a] Thermal corrections at the structure optimisation levels are used.

index of bond formation at the transition state, one can roughly estimate the *d* value for *p*-nitrostyrene as 0.70 by multiplying the *d* value (0.74) by 2.28/2.40 taking the mean distance of C1–O1 for the styrenes other than *p*-nitrostyrene as 2.28 Å (in the case of B3LYP/LanL2DZ optimised structure, see Table 2). The value 0.70 well agrees with the value adopted to correct the deviation of *p*-nitrostyrene in the FMO plot (Fig. 2).

The calculated free energies of activation ($\Delta G^{\ddagger}$) at the levels of B3LYP/6-311+G(d,p)//B3LYP/LanL2DZ and B3LYP/6-311+G(d,p)//B3LYP/6-31G(d) are shown in Table 3. In order to review the linear free energy relationship, the plots of log k_2 *vs.* $-\Delta G^{\ddagger}$ are drawn in Fig. 3 together with that of the experimental $\Delta G^{\ddagger}$ (see also Table 5). Although the calculations at both levels give excellent straight lines, considerable discrepancies are observed in the exact values of $\Delta G^{\ddagger}$ and the slopes between theory and experiment. These apparent discrepancies prompted us to undertake further investigation.

DFT calculations including a quaternary ammonium ion

A reason for the disagreement between the theoretical and experimental $\Delta G^{\ddagger}$ values may be attributed to the electrostatic effect of the quaternary ammonium ion, which was not

Table 4 Activation parameters calculated including a tetraethylammonium ion (in kJ mol^{-1} or J mol^{-1} K^{-1})

	B3LYP/LanL2DZ // B3LYP/LanL2DZ			B3LYP/6-311+G(d,p) // B3LYP/LanL2DZ			B3LYP/6-31G(d) // B3LYP/6-31G(d)			B3LYP/6-311+G(d,p) // B3LYP/6-31G(d)		
X	$\Delta H^{\ddagger}$	$\Delta S^{\ddagger}$	$\Delta G^{\ddagger a}$	$\Delta H^{\ddagger b}$	$\Delta G^{\ddagger a,b}$	$\Delta E^{\ddagger c}$	$\Delta H^{\ddagger}$	$\Delta S^{\ddagger}$	$\Delta G^{\ddagger a}$	$\Delta H^{\ddagger b}$	$\Delta G^{\ddagger a b}$	$\Delta E^{\ddagger c}$
p-Me	13.0	−187	68.6	23.6	79.3	21.5	29.9	−197	88.5	34.6	93.3	32.1
H	11.0	−175	63.2	21.2	73.4	19.5	28.0	−183	82.6	32.2	86.9	30.1
p-Cl	6.5	−173	58.2	17.2	68.9	15.2	24.9	−187	80.6	28.1	83.8	25.5
m-Cl	7.6	−179	61.1	17.7	67.0	15.3	25.2	−192	82.3	28.1	85.3	25.6
m-Br	7.9	−166	57.3	17.6	71.2	15.8	17.5	−200	77.0	29.0	88.5	27.5
3,4-diCl	3.0	−181	56.9	14.0	67.9	11.8	22.3	−191	79.2	24.8	81.7	22.1
m-NO2	0.1	−162	48.5	13.0	61.4	11.7	13.0	−191	69.9	18.9	75.8	18.0
p-NO_2	−6.0	−173	45.6	6.7	58.3	4.9	6.9	−203	67.5	15.1	75.7	12.7

[a] At 298.15 K. [b] Calculated based on thermal corrections of geometry optimization. [c] Relative energies calculated using electronic energies without any thermal corrections.

Table 5 Experimental activation parameters (in kJ mol^{-1} K or J mol^{-1} K^{-1})[a]

	Experimental		
X	$\Delta H^{\ddagger}$	$\Delta S^{\ddagger}$	$\Delta G^{\ddagger b}$
p-Me	20.3 ± 0.7	−177 ± 3	73.2
H	18.8 ± 1.5	−181 ± 5	72.7
p-Cl	15.9 ± 1.2	−185 ± 4	70.9
m-Cl	18.0 ± 1.5	−178 ± 5	71.0
m-Br	17.5 ± 1.1	−178 ± 4	70.7
3,4-diCl	10.7 ± 0.7	−199 ± 3	69.9
m-NO2	11.4 ± 1.4	−195 ± 5	69.4
p-NO_2	15.6 ± 1.7	−173 ± 6	67.2

[a] Obtained from Eyring plots. [b] Calculated at 298.15 K.

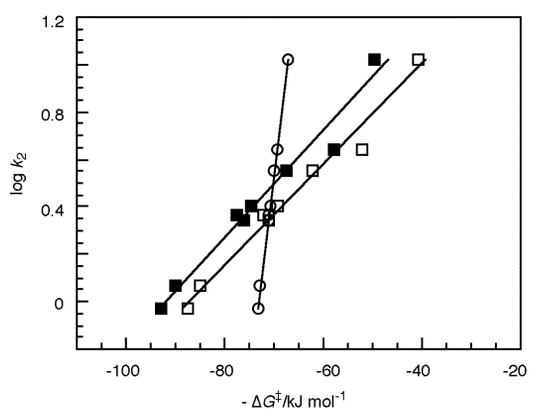

Fig. 3 Plots of log k_2 *vs.* $-\Delta G^{\ddagger}$ calculated at the B3LYP/6-311+G(d,p) level on the structures optimised at the levels indicated below. The quaternary ammonium ion is not included in the calculations. ■: B3LYP/6-31G(d) (r = 0.98), □: B3LYP/LanL2DZ (r = 0.99), ○: experimental (r = 1.0).

incorporated into the above calculations. We noted the marked inconsistency in the slopes of the plots observed between experiment and theory (Fig. 3). It has been known that a quaternary ammonium permanganate exists as an ion pair in CH_2Cl_2 solutions.[2d] Since in the transition states the negative charge of the permanganate ion moiety is spread over the styrene moiety, the energy stabilization of the transition states caused by ion pairing with Et_4N^+ would be expected to be smaller than that of ground state $Et_4N^+MnO_4^-$. This fact would raise the actual activation energy especially for the reaction of electron-withdrawing styrenes. Therefore, calculations using a more extensive model and taking into account ion pairing with Et_4N^+ would result in a larger slope for the plot of log k_2 *vs.* $-\Delta G^{\ddagger}$ than those observed in Fig. 3.

We performed optimizations of the reactants and transition structures including a tetraethylammonium ion and calculated $\Delta G^{\ddagger}$ as well as $\Delta S^{\ddagger}$ and $\Delta H^{\ddagger}$ using the same theoretical procedure as described above. The results are indicated in Table 4. The experimental activation parameters obtained from Eyring plots over the temperature range from 15.0 to 30.0 °C are also indicated in Table 5. It can be noted that the large negative values of the experimental $\Delta S^{\ddagger}$ are well reproduced at both levels of calculations. The plots of log k_2 *vs.* $-\Delta G^{\ddagger}$ at B3LYP/6-311+G(d,p)//B3LYP/LanL2DZ and B3LYP/6-311+G(d,p)//B3LYP/6-31G(d) are shown in Fig. 4 together with that of the experimental $\Delta G^{\ddagger}$.

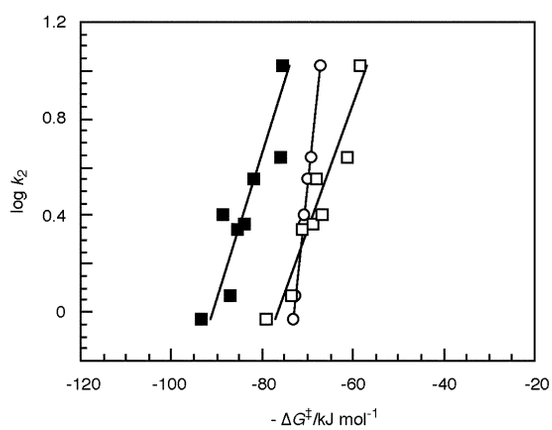

Fig. 4 Plots of log k_2 *vs.* $-\Delta G^{\ddagger}$ at B3LYP/6-311+G(d,p) level on the structures optimised at the levels below indicated. The quaternary ammonium ion is incorporated in the calculations. ■: B3LYP/6-31G(d) (r = 0.89), □: B3LYP/LanL2DZ (r = 0.96), ○: experimental (r = 1.0).

It can be seen that the slopes of the plots in Fig. 4 has been significantly improved at both levels of calculation compared to those in Fig. 3, as expected above from the electrostatic effect of the quaternary ammonium ion. The exact values of $\Delta G^{\ddagger}$ calculated with 6-311+G(d,p) basis set on the LanL2DZ optimised structures are in good agreement with the experimental values, while those calculated on the 6-31G(d) optimised structures are considerably deviated from the experimental values. Furthermore, it should be noted that the differences in calculated $\Delta G^{\ddagger}$ due to the level of geometry optimization was enlarged compared to the calculations without the quaternary ammonium ion. Nearly the same differences were observed between the relative energies ($\Delta E^{\ddagger}$, see Table 4) obtained from electronic energies without any thermal corrections. This fact suggests that the differences are derived mainly from electronic energies but not from frequencies and thermal corrections.

The optimized structures of the transition state with the counter ion are given in Fig. 5, as well as the optimised geometry of $Et_4^+MnO_4^-$ in Fig. 6, with some geometrical figures and summed atomic charges of three components calculated at the level of 6-311+G(d,p) on the LanL2DZ and 6-31G(d) optimized structures, respectively. It can be seen that the differences

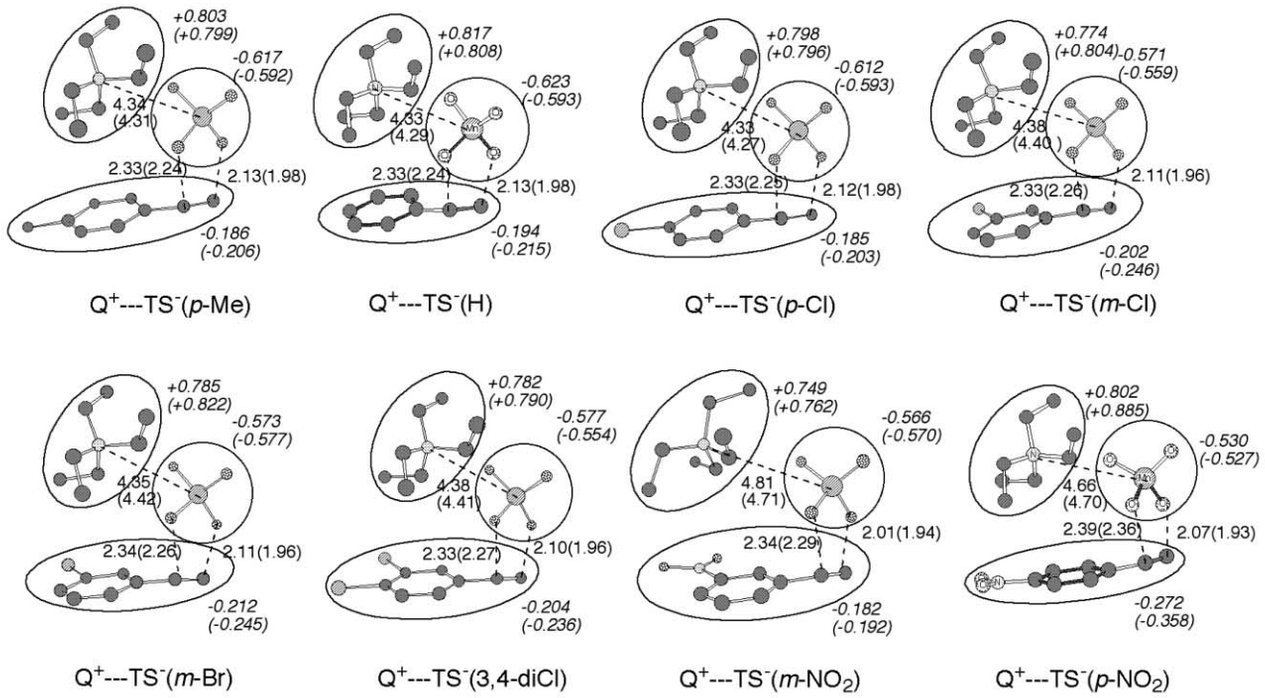

Fig. 5 Geometries of the transition states optimised at the level of B3LYP/LanL2DZ with the counter cation (hydrogen atoms are omitted for easy seeing). Figures in roman refer to the interatomic distance (Å) specified by a dotted line. Figures in italic refer to the total atomic charge for the component parts surrounded by a circle. The figures in parentheses are those for the B3LYP/6-31G* optimised geometries.

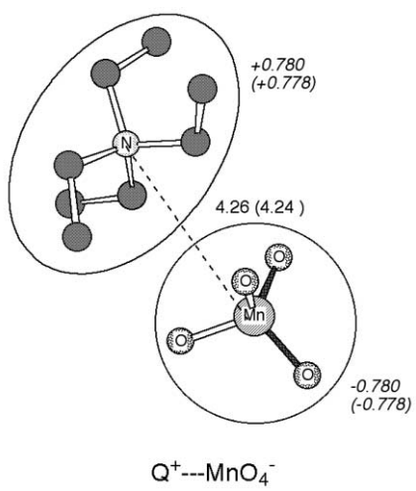

Fig. 6 Geometry of the permanganate ion with a counter ion. See the caption of Fig. 5 for what the figures refer to.

in the C–O bond distances due to the level of optimization are larger than those in the transition structures calculated without the counter ion (see Table 2), especially for C1–O1. Furthermore, considerable differences in the negative charges on styrene parts are noted between the levels of optimization. These factors may have worked for the LanL2DZ optimization to be favored for giving the results closer to experiments.

Conclusions

A comparison between the results of experimental and theoretical studies for the substituent effects of permanganate oxidation of styrene derivatives in CH_2Cl_2 with tetaethylammmonium ion as a phase catalyst has been accomplished. The [3 + 2] transition states have been optimised in the form of an ion pair with a quaternary ammonium ion using DFT calculation. The free energies of activation as well as the activation entropies computed for these models at the level of B3LYP/6-311+G(d,p)//B3LYP/LanL2DZ are in good agreement with those obtained from kinetic experiments. To the best of our knowledge, this is the first report where full activation parameters have been compared between experiment and theory for the permanganate oxidation of alkenes. The experimental results were also analysed by semi-quantitative frontier molecular orbital treatments. The more reactant-like geometry of the transition state predicted for the reaction of *p*-nitrostyrene from the deviation from the straight line of the semi-quantitative FMO plot is in good agreement with that optimised by the DFT calculation.

Acknowledgements

Most of the calculations were performed on the workstations of the Computer Laboratory of the Graduate School of Science and Technology, Niigata University. The authors would like to express their gratitude to the staff of the laboratory for providing us with computer capabilities.

References

1 (*a*) G. Wagner, *J. Russ. Phys. Chem. Soc.*, 1895, **27**, 219; (*b*) K. B. Wiberg and K. A. Saegebarth, *J. Am. Chem. Soc.*, 1957, **79**, 2822; (*c*) R. Stewart, *Oxidation in Organic Chemistry Part A*, ed. K. B. Wiberg, Academic Press, New York, 1965, pp. 1–68.
2 (*a*) F. Freeman, C. O. Fuselier and E. M. Karchefski, *Tetrahedron Lett.*, 1975, 2133; (*b*) F. Freeman, C. O. Fuselier, C. R. Armstead, C. E. Dalton, P. A. Davidson, E. M Karchefski, D. E. Krochman, E. M. Johnson and N. K. Jones, *J. Am.Chem. Soc.*, 1981, **103**, 1154; (*c*) F. Freeman and J. C. Kappos, *J. Am.Chem. Soc.*, 1985, **107**, 6628; (*d*) D. G. Lee and K. C. Brown, *J. Am. Chem. Soc.*, 1982, **104**, 5076; (*e*) J. F. Perez-Benito and D. G. Lee, *J. Org. Chem.*, 1987, **52**, 3239; (*f*) T. Ogino and N. Kikuiri, *J. Am. Chem. Soc.*, 1989, **111**, 6174; (*g*) T. Ogino, K. Hasegawa and E. Hoshino, *J. Org. Chem.*, 1990, **55**, 2653.
3 K. Fukui, *Bull. Chem. Soc. Jpn.*, 1966, **39**, 498.
4 (*a*) J. S. Littler, *Tetrahedron*, 1971, **27**, 81; (*b*) F. Freeman, *Chem. Rev.*, 1975, **75**, 439.
5 K. B. Sharpless, A. Y. Teranishi and J-E. Bäckvall, *J. Am. Chem. Soc.*, 1977, **99**, 3120.
6 (*a*) K. A. Jørgensen and R. Hoffmann, *J. Am. Chem. Soc.*, 1986, **108**, 1867; (*b*) Y-D. Wu, Y. Wang and K. N. Houk, *J. Org Chem.*, 1992, **57**, 1362; (*c*) E. J. Corey and M. C. Noe, *J. Am. Chem. Soc.*, 1993,

115, 12579; (*d*) E. J. Corey and M. C. Noe, *J. Am. Chem. Soc.*, 1996, **118**, 11038; (*e*) E. J. Corey, M. C. Noe and M. J. Grogan, *Tetrahedron Lett.*, 1996, **28**, 4899; (*f*) J. Haller, T. Strassner and K. N. Houk, *J. Am. Chem. Soc.*, 1997, **119**, 8031; (*g*) A. J. DelMonte, J. Haller, K. N. Houk, K. B. Sharpless, D. A. Singleton, T. Strassner and A. A. Thomas, *J. Am. Chem. Soc.*, 1997, **119**, 9907.

7 T. Ogino, T. Watanabe, M. Matsuura, C. Watanabe and H. Ozaki, *J. Org. Chem.*, 1998, **63**, 2627.

8 (*a*) N. K. Houk and Th. Strassner, *J. Org. Chem.*, 1999, **64**, 800; (*b*) Th. Strassner and M. Busold, *J. Org. Chem.*, 2001, **66**, 672.

9 (*a*) S. Dapprich, G. Ujaque, F. Maseras, A. Lledós, D. G. Musaev and K. Morokuma, *J. Am. Chem. Soc.*, 1996, **118**, 11660; (*b*) U. Pidun, C. Boehme and G. Frenking, *Angew. Chem., Int. Ed. Engl.*, 1996, **35**, 2817; (*c*) M. Torrent, L. Deng, M. Duran, M. Sola and T. Ziegler, *Organometallics*, 1997, **16**, 13.

10 (*a*) D. G. Lee, K. C. Brown and H. Karaman, *Can. J. Chem.*, 1986, **64**, 1054; (*b*) F. Freeman and K. Kappos, *J. Org. Chem.*, 1989, **54**, 2730; (*c*) H. B. Henbest, W. R. Jackson and B. C. G. Rob, *J. Chem. Soc. (B)*, 1966, 803.

11 C. G. Overberger, J. H. Saunders, R. E. Allen and R. Gander, *Org. Synth., Coll. Vol. II*, 1955, 200.

12 (*a*) A. D. Becke, *J. Chem. Phys.*, 1993, **98**, 5648; (*b*) A. D. Becke, *Phys. Rev.*, 1988, **A38**, 3098.

13 M. J. Frisch, G. W. Trucks, H. B. Schlegel, G. E. Scuseria, M. A. Robb, J. R. Cheeseman, V. G. Zakrzewski, J. A. Montgomery, Jr., R. E. Stratmann, J. C. Burant, S. Dapprich, J. M. Millam, A. D. Daniels, K. N. Kudin, M. C. Strain, O. Farkas, J. Tomasi, V. Barone, M. Cossi, R. Cammi, B. Mennucci, C. Pomelli, C. Adamo, S. Clifford, J. Ochterski, G. A. Petersson, P. Y. Ayala, Q. Cui, K. Morokuma, D. K. Malick, A. D. Rabuck, K. Raghavachari, J. B. Foresman, J. Cioslowski, J. V. Ortiz, A. G. Baboul, B. B. Stefanov, G. Liu, A. Liashenko, P. Piskorz, I. Komaromi, R. Gomperts, R. L. Martin, D. J. Fox, T. Keith, M. A. Al-Laham, C. Y. Peng, A. Nanayakkara, M. Challacombe, P. M. W. Gill, B. Johnson, W. Chen, M. W. Wong, J. L. Andres, C. Gonzalez, M. Head-Gordon, E. S. Replogle and J. A. Pople, *GAUSSIAN 98, Revision A.9*, Gaussian, Inc., Pittsburgh PA, 1998.

14 W. R. Wadt and P. J. Hay, *J. Chem. Phys.*, 1985, **82**, 284.

15 M. W. Wong, *Chem. Phys. Lett.*, 1996, **256**, 391.

16 J. J. P. Stewart, *J. Comput. Chem.*, 1989, **10**, 209.

17 PM3(tm) is a modification of the original PM3[16] including a parametrization for transition metals.

18 Wavefunction Inc., Irvine, CA, USA.

19 (*a*) M. J. S. Dewar, *J. Am. Chem. Soc.*, 1952, **74**, 3341; (*b*) G. Klopman, *J. Am. Chem. Soc.*, 1968, **90**, 223; see also *Chemical Reactivity and Reaction Paths*, ed. G. Klopman, Wiley, New York, 1974, 55–165.